Ab initio many-body perturbation theory and no-core shell model*

B. S. Hu(胡柏山) Q. Wu(吴强) F. R. Xu(许甫荣)[1)]

State Key Laboratory of Nuclear Physics and Technology, School of Physics, Peking University, Beijing 100871, China

Abstract: In many-body perturbation theory (MBPT) we always introduce a parameter $N_{\rm shell}$ to measure the maximal allowed major harmonic-oscillator (HO) shells for the single-particle basis, while the no-core shell model (NCSM) uses $N_{\rm max}\hbar\Omega$ HO excitation truncation above the lowest HO configuration for the many-body basis. It is worth comparing the two different methods. Starting from "bare" and Okubo-Lee-Suzuki renormalized modern nucleon-nucleon interactions, $\rm NNLO_{opt}$ and JISP16, we show that MBPT within Hartree-Fock bases is in reasonable agreement with NCSM within harmonic oscillator bases for ^{4}He and ^{16}O in "close" model space. In addition, we compare the results using "bare" force with the Okubo-Lee-Suzuki renormalized force.

Keywords: MBPT, NCSM, Okubo-Lee-Suzuki, nuclear force

PACS: 21.60.De, 21.30.Fe, 21.10.Dr **DOI:** 10.1088/1674-1137/41/10/104101

1 Introduction

The *ab initio* description of atomic nuclei is a fundamental and challenging problem in nuclear structure theory. *Ab initio* methods, such as the no-core shell-model (NCSM) [1–3], the Green's function Monte Carlo approach [4–7], and the coupled-cluster (CC) method [8–10], have been used to madk great progress in exploring the structure of atomic nuclei in the past decade. However, all these models are computationally demanding, which leads to a hard limitation on the number of nucleons that can be handled. For heavier nuclei there are a few *ab initio* approaches that can calculate the structure of closed-shell nuclei or those nearby, such as the CC method, importance-truncated no-core shell model (IT-NCSM) [11, 12] and many-body perturbation theory (MBPT) in Hartree-Fock (HF) basis [13–15]. However, there are some other methods [16–22] that can give good descriptions of the heavier nuclei. *Ab initio* methods always use a Slater-determinant basis constructed from harmonic-oscillator (HO) single-particle states. The limitation of computer power requires that the Schrödinger equation is solved in a model space with a finite number of configurations or basis states. The CC and MBPT approaches always use $N_{\rm shell}$ major shell truncation at single-particle level, while NCSM uses $N_{\rm max}$ model space truncation at many-body total energy level. The HF state is taken as the reference state for the CC and MBPT approaches, to accelerate convergence and cancel some single excitations of the intermediate states, while the NCSM is always calculated in HO basis. We will compare the results using different truncations in MBPT and NCSM calculations with the same effective Hamiltonian.

Two modern interactions, $\rm NNLO_{opt}$ [23] and JISP16 [24–26], are used in our MBPT and NCSM calculations. The new NN chiral interaction $\rm NNLO_{opt}$ yields $\chi^2\approx1$ per degree of freedom for laboratory energies below approximately 125 MeV by using the optimization tool, Practical Optimization Using No Derivatives (for Squares) algorithm, with respect to phase-shift analysis. The JISP16 interaction is obtained by phase-equivalent transformations of the J-matrix inverse scattering potential to describe not only the NN data but the binding energies and spectra of nuclei with $A\leqslant16$. It has been demonstrated [23, 26] that many aspects of nuclear structure can be understood in terms of these NN interactions, without resorting to three-body forces. Another similarity of these two interactions is that they are "soft" and can be used directly in the *ab initio* calculation without renormalization. They can provide a fast convergence for *ab initio* calculations. In practice, if we expand these "bare" interactions in a small HO model space with low oscillator parameter $\hbar\Omega$, the momentum cutoff λ of the employed nuclear interactions may exceed the ultraviolet (UV) momentum associated with the energy of the highest HO level [27, 28],

$$\Lambda_{\rm UV}\equiv\sqrt{2(N+3/2)}\hbar/b. \quad (1)$$

Received 16 May 2017

* Supported by National Key Basic Research Program of China (2013CB834402), National Natural Science Foundation of China (11235001, 11320101004, 11575007) and the CUSTIPEN (China-U.S. Theory Institute for Physics with Exotic Nuclei) funded by the U.S. Department of Energy, Office of Science (DE-SC0009971)

1) E-mail: frxu@pku.edu.cn

Here, $N=(2n+l)$ denotes the HO shells, $n(l)$ is the radial (angular-momentum) quantum number, $b\equiv\sqrt{\hbar/(m\Omega)}$ is the HO length, and m is the nucleon mass. Then, we cannot get converged nuclear structure results in this small model space. For example, when we choose $N=9$ and $\hbar\Omega=10$ MeV for HO basis, the model space $\Lambda_{\rm UV}\approx 444$ MeV/c is smaller than the momentum cutoff $\lambda\approx 500\sqrt{2}$ MeV/c of JISP16 in Ref. [29]. In order to speed up convergence with lower model space UV momentum, we can decrease the momentum cutoff of the original interaction by a renormalization scheme specified by a renormalization group transformation or a similarity transformation. Such transformations preserve all experimental quantities up to the low momentum cutoff domain. The Okubo-Lee-Suzuki (OLS) technique [2, 30–35] is a universal renormalization method and always improves the results with the "bare" interaction, in particular, for smaller spaces and lower oscillator parameter $\hbar\Omega$ [36]. We will compare the results using the "bare" nuclear force with those using the OLS renormalized force.

The main purpose of this paper is to compare the ground-state properties of doubly closed-shell nuclei calculated by different many-body methods, MBPT and NCSM, with different effective Hamiltonians, "bare" and OLS renormalized nuclear interactions. The paper is organized as follows. In Section 2 we give an outline of the derivation for the effective Hamiltonian. In Section 3 we give the details of our many-body calculations, present our results and compare them. A summary and outlook is given in Section 4.

2 Effective Hamiltonian and decoupling operator

Starting from an arbitrary Hamiltonian H with the eigensystem E_k, $|k\rangle$,

$$H|k\rangle=E_k|k\rangle, \tag{2}$$

we can divide the full Hilbert space into a model space and its complement by defining two projection operators P and Q with $P+Q=1$, $P^2=P$, $Q^2=Q$ and $PQ=0$. The goal of calculating the effective Hamiltonian is to reproduce exactly the eigenvalues and any observable characterized by an operator in model space. The similarity transformation can achieve this purpose [32],

$$\mathcal{H}{\rm e}^{-G}|k\rangle=({\rm e}^{-G}H{\rm e}^{G})({\rm e}^{-G}|k\rangle)=E_k({\rm e}^{-G}|k\rangle), \tag{3}$$

where $\exp(G)\exp(-G)=1$. The transformed Hamiltonian $\mathcal{H}$ can be decomposed into four terms,

$$\mathcal{H}=P\mathcal{H}P+P\mathcal{H}Q+Q\mathcal{H}P+Q\mathcal{H}Q. \tag{4}$$

If we define the effective Hamiltonian $H_{\rm eff}$ in model space as

$$H_{\rm eff}=P\mathcal{H}P=P{\rm e}^{-G}H{\rm e}^{G}P, \tag{5}$$

we need the decoupling condition.

$$Q\mathcal{H}P=Q{\rm e}^{-G}H{\rm e}^{G}P=0. \tag{6}$$

If ${\rm e}^{G}$ is a solution of Eq. (6), we can easily see that the eigenvalues of $H_{\rm eff}$ agree with the H in model space. The correlation operator G cannot be determined uniquely from the above decoupling condition. The unique solution is obtained from the restrictions [33],

$$PGP=QGQ=0. \tag{7}$$

In nuclear physics, the Lee-Suzuki approach that chooses the correlation operator ω as G has been very widely used, especially for some nuclear interaction renormalization schemes, such as the effective low-momentum NN interaction $V_{\rm low\text{-}k}$ and the OLS renormalization scheme. We will mainly discuss the OLS method.

2.1 Lee-Suzuki approach

Let us choose ${\rm e}^{G}={\rm e}^{\omega}$, where the operator ω acts as a mapping between the P and Q spaces [35], i.e.,

$$|q\rangle=\omega|p\rangle,\quad (|p\rangle\in P|k\rangle,|q\rangle\in Q|k\rangle). \tag{8}$$

We can easily find

$$\begin{aligned}&\omega=Q\omega P,\\&Q\omega Q=P\omega P=P\omega Q=0,\\&\omega^2=\omega^3=\omega^4=...=0,\\&{\rm e}^{\omega}=1+\omega,\\&{\rm e}^{-\omega}=1-\omega.\end{aligned} \tag{9}$$

The decoupling condition Eq. (6) is satisfied. So the eigenvalues of $H_{\rm eff}$ agree with the H in model space. Let us denote the model space basis states as α_P, and its complement Q-space states as α_Q. Using the first expression in Eq. (9), the action of the transformation operator ω on $|k\rangle$ is 510

$$\langle\alpha_Q|k\rangle=\sum_{\alpha_P}\langle\alpha_Q|\omega|\alpha_P\rangle\langle\alpha_P|k\rangle. \tag{10}$$

If the model space has d_P dimensions, we can choose a set κ of $\{|k\rangle\}_{d_P\times d_P}$. The matrix elements of ω can be found in a noniterative scheme,

$$\langle\alpha_Q|\omega|\alpha_P\rangle=\sum_{k\in\kappa}\langle\alpha_Q|k\rangle\langle\tilde{\rm k}|\alpha_P\rangle, \tag{11}$$

where $\langle\tilde{\rm k}|\alpha_P\rangle$ denote the inverted matrix of $\langle\alpha_P|k\rangle$, i.e. $\sum\limits_{\alpha_P}\langle\tilde{\rm k}|\alpha_P\rangle\langle\alpha_P|k'\rangle=\delta_{kk'}$, for $k,k'\in\kappa$.

Then, we can easily get the effective Hamiltonian $\tilde{\rm H}_{\rm eff}$ in model space as

$$\tilde{H}_{\rm eff}=P{\rm e}^{-G}H{\rm e}^{G}P=P(1-\omega)H(1+\omega)P. \tag{12}$$

However, the transformation e^{ω} is not unitary, and the effective Hamiltonian $\tilde{H}_{\rm eff}$ is non-Hermitian. Unitarity can be achieved using the anti-Hermitian operator G=arctanh$(\omega-\omega^{\dagger})$ ($G^{\dagger}=-G$), and the Hermitian effective Hamiltonian $\bar{H}_{\rm eff}$ defined on the model space P is given by [3, 32, 33]

$$\begin{aligned}\bar{H}_{\rm eff} &= [P(1+\omega^{\dagger}\omega)P]^{1/2}\\ &\quad\times PH(P+Q\omega P)[P(1+\omega^{\dagger}\omega)P]^{-1/2}. \end{aligned}\tag{13}$$

The $\bar{H}_{\rm eff}$ can also be rewritten as

$$\begin{aligned}\bar{H}_{\rm eff} &= [P(1+\omega^{\dagger}\omega)P]^{-1/2}\\ &\quad\times(P+P\omega^{\dagger}Q)H(P+Q\omega P)\\ &\quad\times[P(1+\omega^{\dagger}\omega)P]^{-1/2}. \end{aligned}\tag{14}$$

With the help of the solution of Eq. (11) for ω we can get the matrix elements of $\bar{H}_{\rm eff}$,

$$\begin{aligned}\langle\alpha_P|\bar{H}_{\rm eff}|\beta_P\rangle &= \sum_{k\in\kappa}\sum_{\alpha_{P'}}\sum_{\beta_{P'}}\langle\alpha_P|(1+\omega^{\dagger}\omega)^{-1/2}|\alpha_{P'}\rangle\\ &\quad\times\langle\alpha_{P'}|\tilde{\rm k}\rangle E_k\langle\tilde{\rm k}|\beta_{P'}\rangle\\ &\quad\times\langle\beta_{P'}|(1+\omega^{\dagger}\omega)^{-1/2}|\beta_{P'}\rangle. \end{aligned}\tag{15}$$

To compute the elements of $(1+\omega^{\dagger}\omega)^{-1/2}$, we can use the relation,

$$\begin{aligned}\langle\alpha_P|(1+\omega^{\dagger}\omega)|\alpha_{P'}\rangle &= \langle\alpha_P|(1+\omega^{\dagger})(1+\omega)|\alpha_{P'}\rangle\\ &= \sum_{k\in\kappa}\langle\alpha_P|\tilde{\rm k}\rangle\langle\tilde{\rm k}|\alpha_{P'}\rangle. \end{aligned}\tag{16}$$

2.2 Renormalization methods to soften realistic interactions

Realistic NN potentials, such as CD-Bonn [37], Nijmegen [38], Argonne V18 (AV18) [39], INOY [40], and, to some extent, the chiral N^{3}LO [41, 42], generate strong short-range correlations, so none of them can be used directly in nuclear structure calculations without renormalization or a large-enough truncated harmonic-oscillator (H.O.) basis. In order to solve this problem and to speed up convergence, we need a renormalization scheme. A traditional approach is to introduce the reaction matrix G (G-matrix) in the Brueckner-Bethe-Goldstone theory [43–45]. Recently, a new class of these schemes has been developed, including $V_{\rm low\text{-}k}$ [46, 47], similarity renormalization group (SRG) [48], Okubo-Lee-Suzuki [30–35], and the unitary correlation operator method (UCOM) [49, 50]. These renormalization schemes soften the interactions and generate effective Hamiltonians, while they preserve all experimental quantities in the low-energy domain.

2.2.1 Effective low-momentum NN interaction $V_{\rm low\text{-}k}$

Realistic NN potentials always generate strong short-range correlations, so their momentum space matrices $V(k,k')$ are still significant at high momentum transfer. If the troublesome high-momentum modes can be eliminated in a physically equivalent way, we can get soft nuclear interactions. By introducing a cutoff in momentum space, we can separate the Hilbert space into a low momentum and a high momentum part. The renormalization group (RG) can be used to construct the effective interaction $V_{\rm low\text{-}k}$ in the low momentum space. The evolved effective interaction $V_{\rm low\text{-}k}$ is energy-independent and preserves two-nucleon observables for relative momenta up to the cutoff. Bogner, Kuo and Schwenk [47] have shown that the low-momentum Hamiltonian obtained from the solution of the RG eqution is equivalent to the effective theory derived using Bloch-Horowitz or Lee-Suzuki projection methods. We will discuss the Lee-Suzuki projection method.

The Lee-Suzuki approach has been outlined in Section 2.1. For a given partial wave, the P and Q are defined in a continuous plane wave basis as

$$\begin{aligned}P &= \frac{2}{\pi}\int_0^{\Lambda} p^2{\rm d}p|p\rangle\langle p|,\\ Q &= \frac{2}{\pi}\int_{\Lambda}^{\infty} q^2{\rm d}q|q\rangle\langle q|. \end{aligned}\tag{17}$$

Then we can get the effective low-momentum Hamiltonian,

$$\begin{aligned}\bar{H}^{\rm LS}_{\rm low\text{-}k} &= [P(1+\omega^{\dagger}\omega)P]^{1/2}\\ &\quad\times PH(P+Q\omega P)[P(1+\omega^{\dagger}\omega)P]^{-1/2}. \end{aligned}\tag{18}$$

2.2.2 Okubo-Lee-Suzuki renormalization

The intrinsic Hamiltonian of the A-nucleon system used in this work reads

$$\hat{H}_{\rm int}=\sum_{i<j}^{A}\frac{(\vec{p}_i-\vec{p}_j)^2}{2mA}+\sum_{i<j}^{A}V_{NN,ij}.\tag{19}$$

Here, the first term on the right is the intrinsic kinetic energy, and V_{NN} is the NN interaction including the Coulomb interaction between protons.

We modify the intrinsic Hamiltonian by adding the center-of-mass (c.m.) harmonic-oscillator (HO) Hamiltonian,

$$H^{\Omega}_{\rm c.m.}=\frac{\vec{P}^2}{2mA}+\frac{1}{2}Am\Omega^2\vec{R}^2\tag{20}$$

with the nucleon mass m, $\vec{P}=\sum_{i=1}^{A}\vec{p}_i$ and $\vec{R}=(1/A)\sum_{i=1}^{A}\vec{r}_i$.

The modified Hamiltonian can then be written as

$$\begin{aligned}H^{\Omega}_{A} &= H_{\rm int}+H^{\Omega}_{\rm c.m.}=\sum_{i=1}^{A}\left[\frac{\vec{p}_i^{\,2}}{2m}+\frac{1}{2}m\Omega^2\vec{r}_i^{\,2}\right]\\ &\quad+\sum_{i<j}^{A}\left[V_{NN,ij}-\frac{m\Omega^2}{2A}(\vec{r}_i-\vec{r}_j)^2\right]. \end{aligned}\tag{21}$$

We can simply write the above Hamiltonian as

$$H_A^\Omega=\sum_{i=1}^{A}h_i+\sum_{i<j}^{A}V_{ij}^{\Omega,A}. \tag{22}$$

Okubo-Lee-Suzuki renormalization is able to accommodate the short-range two-body correlations by choosing the anti-Hermitian operator $G=\text{arctanh}(\omega-\omega^\dagger)$. Using the Lee-Suzuki approach outlined in Section 2.1 we can get the Hermitian effective Hamiltonian $\bar{H}_{\text{eff}}$,

$$\bar{H}_{\text{eff}}^A=\text{e}^{-G}H_A^\Omega\text{e}^G. \tag{23}$$

In general, both G and effective Hamiltonian $\bar{H}_{\text{eff}}^A$ are A-body operators. A non-trivial approximation to $\bar{H}_{\text{eff}}^A$ is to develop an a-body effective Hamiltonian $\bar{H}_{\text{eff}}^a$ from the a-body cluster,

$$\begin{aligned}H_a^\Omega &= \sum_{i=1}^{a}\left[\frac{\vec{p}_i^{\,2}}{2m}+\frac{1}{2}m\Omega^2\vec{r}_i^{\,2}\right]\\ &+\sum_{i<j}^{a}\left[V_{NN,ij}-\frac{m\Omega^2}{2A}(\vec{r}_i-\vec{r}_j)^2\right].\end{aligned} \tag{24}$$

Note that in the above cluster Hamiltonian, the strength of the two-body potential $V_{ij}^{\Omega,A}=V_{NN,ij}-\frac{m\Omega^2}{2A}(\vec{r}_i-\vec{r}_j)^2$ depends on the original A. This reflects that the cluster is embedded in the nuclear environment. The effective interaction $\bar{V}_{\text{eff}}^a$ in the a-body cluster approximation for the A-body system is defined as

$$\bar{V}_{\text{eff}}^a=\bar{H}_{\text{eff}}^a-\sum_{i=1}^{a}\left[\frac{\vec{p}_i^{\,2}}{2m}+\frac{1}{2}m\Omega^2\vec{r}_i^{\,2}\right]. \tag{25}$$

Then the A-body problem becomes an approximation to a particular level of clustering with $a\leqslant A$

$$\begin{aligned}\bar{H}_{\text{eff}} &= \sum_{i=1}^{A}\left[\frac{\vec{p}_i^{\,2}}{2m}+\frac{1}{2}m\Omega^2\vec{r}_i^{\,2}\right]\\ &+\frac{(A-a)!(a-2)!}{(A-2)!}\sum_{i_1<i_2\ldots<i_a}^{A}\bar{V}_{\text{eff};i_1\ldots i_a}^a.\end{aligned} \tag{26}$$

We note that there are two ways of convergence. One is that in the limit $a\to A$ and fixed d_P dimension P space, we can obtain the exact solutions for d_P states of the full problem in any finite basis space. Another is that in the limit $P\to 1$ and fixed a-body cluster approximation, we can obtain the exact solutions for an A-nucleon system of the full problem over a very large basis space.

If only NN interactions are included in the A-body system, it is reasonable to expect that a two-body effective interaction would be the most important part of the exact effective interaction. Using the notation of Eq. (22), the two-body effective interaction can be obtained as follows,

$$\begin{aligned}\bar{V}_{\text{eff}}^2 &= P_2\left[\text{e}^{-G_{12}}(h_1+h_2+V_{12}^{\Omega,A})\text{e}^{G_{12}}\right]P_2\\ &-P_2(h_1+h_2)P_2\end{aligned} \tag{27}$$

where $G_{12}=\text{arctanh}(\omega_{12}-\omega_{12}^\dagger)$ and P_2 is a two-nucleon model space projector. As shown in Section 2.1, in order to calculate the $\bar{V}_{\text{eff}}^2$ we need the exact solutions of the Hamiltonian $h_1+h_2+V_{12}^{\Omega,A}$. To be explicit, the two-nucleon calculation is done with

$$\begin{aligned}H_2^{\Omega,A} &= H_{02}+V_{12}^{\Omega,A}\\ &= \frac{\vec{p}^{\,2}}{2m_\mu}+\frac{1}{2}m_\mu\Omega^2\vec{r}^{\,2}+V_{NN}(\vec{r})-\frac{m_\mu\Omega^2}{A}\vec{r}^{\,2},\end{aligned} \tag{28}$$

where $\vec{r}=\vec{r}_1-\vec{r}_2$, $\vec{p}=\frac{\vec{p}_1-\vec{p}_2}{2}$, $m_\mu=\frac{m}{2}$ and $H_{02}=h_1+h_2-H_{2\text{c.m.}}$ differs from h_1+h_2 by subtracting the center-of-mass HO term of nucleons 1 and 2. Then the two-body effective interaction can be obtained as follows,

$$\bar{V}_{\text{eff}}^2=P_2\left[\text{e}^{-G_{12}}(H_{02}+V_{12}^{\Omega,A})\text{e}^{G_{12}}-(H_{02})\right]P_2. \tag{29}$$

Finally, the two-body effective Hamiltonian used in the A-nucleon NCSM calculation becomes

$$\begin{aligned}\bar{H}_{\text{eff}} &= \sum_{i=1}^{A}\left[\frac{\vec{p}_i^{\,2}}{2m}+\frac{1}{2}m\Omega^2\vec{r}_i^{\,2}\right]\\ &+\sum_{i_1<i_2}^{A}\bar{V}_{\text{eff};i_1,i_2}^2-H_{\text{c.m.}}^\Omega+\beta(H_{\text{c.m.}}^\Omega-\frac{3}{2}\hbar\Omega),\end{aligned} \tag{30}$$

where we subtracted the c.m. Hamiltonian $H_{\text{c.m.}}^\Omega$ and added the Lawson projection term $\beta(H_{\text{c.m.}}^\Omega-\frac{3}{2}\hbar\Omega)$ to shift the spurious c.m. excitations.

In MBPT, we only calculate the ground state. We do not need the the Lawson projection term $\beta(H_{\text{c.m.}}^\Omega-\frac{3}{2}\hbar\Omega)$ because the spherical Hartree-Fock method can treat the translational invariance exactly. The following Hamiltonian is used in our MBPT,

$$\begin{aligned}\bar{H}_{\text{eff}} &= \sum_{i_1<i_2}^{A}\left[\frac{(\vec{p}_{i_1}-\vec{p}_{i_2})^2}{2Am}+\frac{m\Omega^2}{2A}(\vec{r}_{i_1}-\vec{r}_{i_2})^2\right]\\ &+\sum_{i_1<i_2}^{A}\bar{V}_{\text{eff};i_1,i_2}^2.\end{aligned} \tag{31}$$

3 Calculations

We use two sets of A-nucleon Hamiltonians in the MBPT and NCSM calculations. One is Eq. (19) with two-body "bare" NNLO_{opt} and JISP16 nuclear interactions in both MBPT and NCSM calculations. The other is Eq. (30) with two-body OLS effective interactions derived from NNLO_{opt} and JISP16 in the MBPT calculation, and Eq. (31) in the NCSM calculation. A detailed description of the MBPT in HF basis was presented in Ref. [51].

For the NCSM calculation, we introduce a many-body basis truncation parameter $N_{\max}$ that is defined as the maximal allowed harmonic-oscillator (HO) excitation above the lowest HO many-body configuration. $N_{\max}$=10 for ^{4}He was chosen, and this means that a total of 11 major HO shells are involved. $N_{\max}$=10 model space in the ^{4}He calculation can allow two nucleons to occupy the $N=5$ HO shell, while the other two nucleons stay in the $N=0$ HO shell. Alternatively, the four nucleons can respectively occupy the $N=1$, 2, 3, 4 HO shells, and so on. The other notable problem for OLS renormalization is that $N_{\rm shell}$ truncation will allow the two active nucleon go to the maximal shell at the same time, so the restriction of the HO single-particle states in P-space is given by $(2n_1+l_1)+(2n_2+l_2)\leqslant 2\times(N_{\rm shell}-1)$.

For ^{16}O, we use $N_{\max}$=8, and this means that a total of 10 major HO shells are involved. We will use the results of MBPT with $N_{\rm shell}$=10 truncation to compare with the NCSM results. For the OLS renormalization to ^{16}O, the $N_{\rm shell}$ truncation requires the HO single-particle states in P-space to satisfy $(2n_1+l_1)+(2n_2+l_2)\leqslant 2\times(N_{\rm shell}-1)$, while $N_{\max}$ truncation satisfied $N_1=(2n_1+l_1)\leqslant(N_{\max}+2)$, $N_2=(2n_2+l_2)\leqslant(N_{\max}+2)$ and $(N_1+N_2)\leqslant(N_{\max}+2)$.

3.1 Application to ^{4}He and ^{16}O

3.1.1 Binding energy

Figures 1, 2, 3 and 4 compare the ground-state energies in the HF approximation, added second- and added third-order MBPT corrections with different nuclear effective interactions for selected closed-shell nuclei. In our MBPT calculations the model space has been extended up to $N_{\rm shell}=10$. We can verify that this truncation is sufficient to ensure that the HF, second-order and third-order MBPT results do not significantly depend on the variation of the oscillator parameter $\hbar\Omega$ when it is

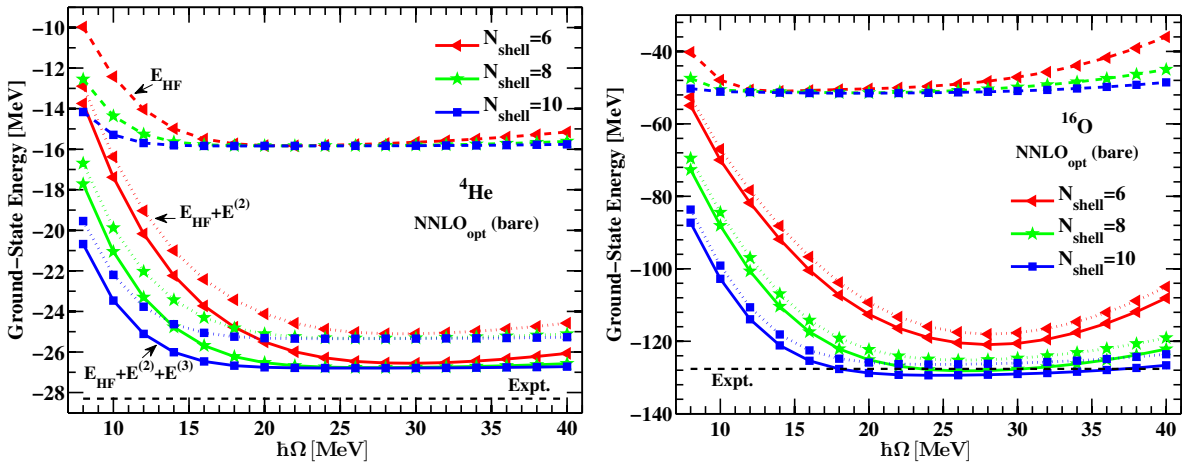

Fig. 1. (color online) Ground-state energies of ^{4}He and ^{16}O as a function of oscillator parameter $\hbar\Omega$ in MBPT calculations with HF reference energy (long-dashed line), added second- (dashed line) and third-order (solid line) MBPT corrections. The interaction used is the "bare" NNLO$_{\rm opt}$ potential [23].

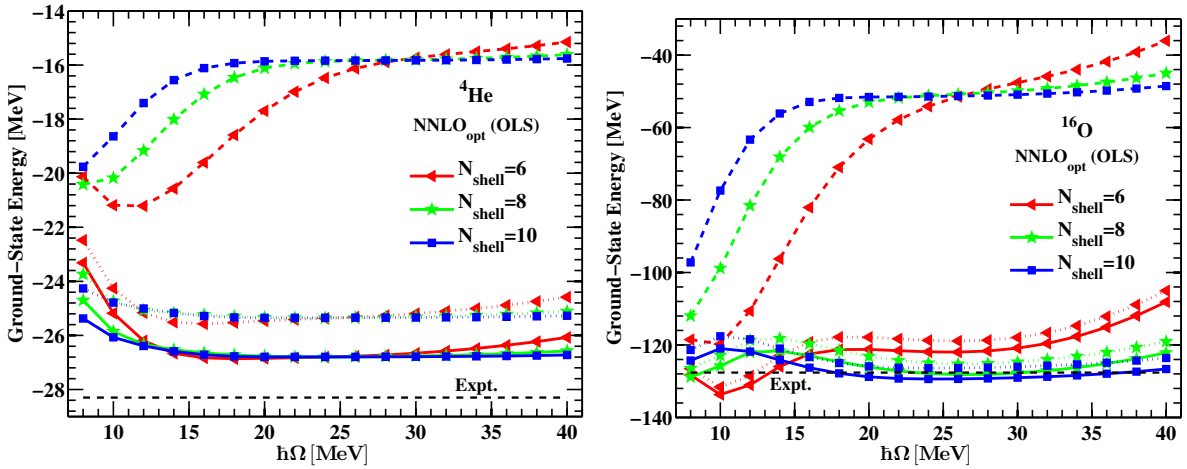

Fig. 2. (color online) Same as Fig. 1 but using OLS effective interaction.

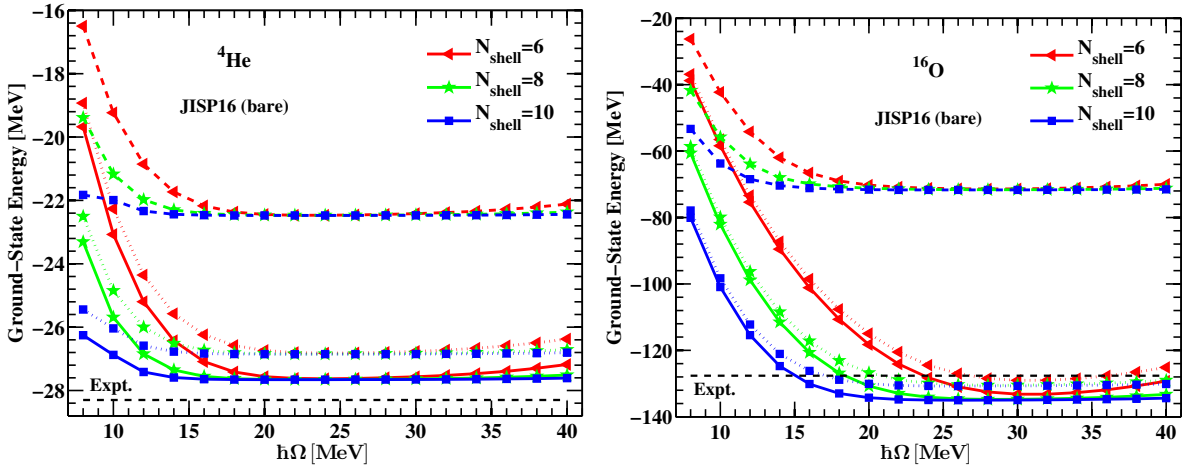

Fig. 3. (color online) Same as Fig. 1 but the interaction used is the "bare" JISP16 potential [24–26].

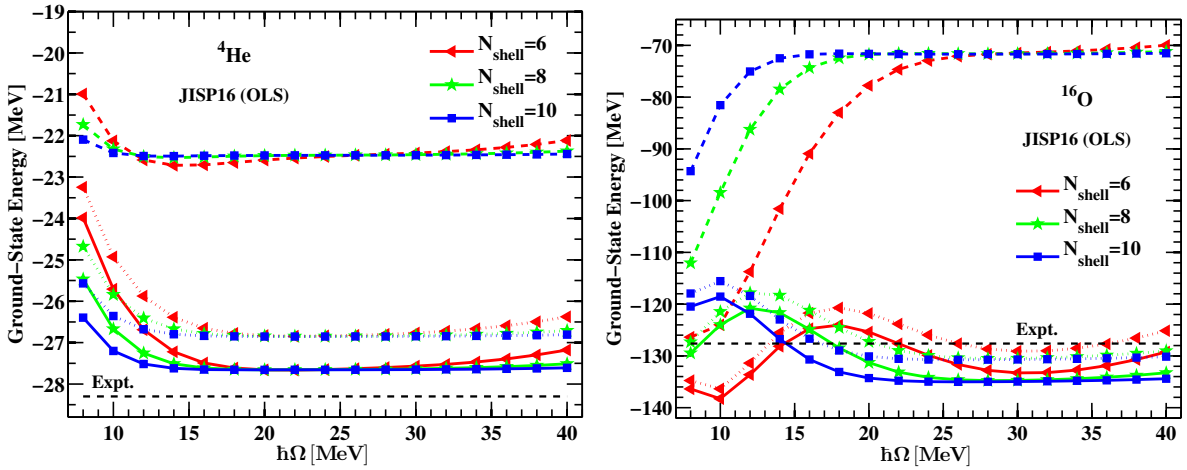

Fig. 4. (color online) Same as Fig. 1 but using OLS effective interaction. The original interaction is the JISP16 potential [24–26].

larger than a certain $\hbar\Omega$, and the convergence with the basis enlargement is fast. For low $\hbar\Omega$ the convergence is slow, and the reason has been shown in Section 1. Our results also show that the convergence of the MBPT expression is fairly rapid, and higher-order corrections are negligible.

Figures 5 and 6 compare the ground-state energies of ^{4}He and ^{16}O as a function of $\hbar\Omega$ in MBPT with $N_{\rm shell}$ major shells truncation at single-particle level and NCSM with $N_{\rm max}$ model space truncation at many-body total energy level. Although these two methods use different model space truncations, $N_{\rm max}$ and $N_{\rm shell}$ truncation, we find that the results of MBPT are in reasonable agreement with NCSM in "close" model space for different nuclear effective interactions. Since third order MBPT can produce too-high binding energies for both interactions based on NCSM results, it seems that 4th order MBPT could be sufficient for the remaining amounts. In NCSM all A nucleons are treated the same, and the $N_{\rm max}$ truncation can generate all possible A-particle A-hole (ApAh) excirations up to the excitation energy $N_{\rm max}\hbar\Omega$ from the unperturbed ground state. But for the MBPT, when we go to the second-order wave function, it includes the $1p1h$, $2p2h$, $3p3h$ and $4p4h$ excitations from the HF reference state, $\phi_{\rm ref}$. When we go to the third-order energy, only the $2p2h$ excitations to ϕ_ν are in fact used:

$$E=E^{(0)}+\Delta E=E^{(0)}+\langle\phi_{\rm ref}|H_{\rm int}|\phi_\nu\rangle \qquad (32)$$

We can find from the IT-NCSM [11] that they can resort to an iterative scheme to generate the $3p3h$ and higher-order configurations when starting with a $0p0h$ single HO Slater determinant reference state.

When looking at the comparison between "bare" force and OLS renormalized force, we find that the two-body OLS effective interaction always improves on the results with bare interaction, in particular, for smaller spaces and lower oscillator parameter $\hbar\Omega$. We can also see that starting at certain $\hbar\Omega$, the results of MBPT or NCSM become the same for the two-body OLS effective

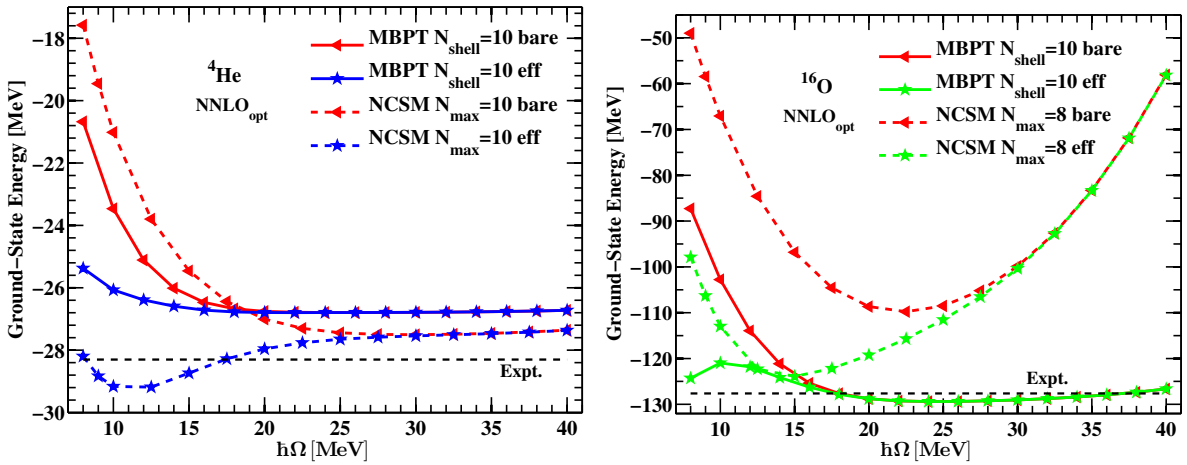

Fig. 5. (color online) Ground-state energies of ^{4}He and ^{16}O as a function of oscillator parameter $\hbar\Omega$ in MBPT and NCSM calculations. The "bare" in this figure denotes using "bare" force, "eff" denotes OLS effective force, "$N_{\rm shell}$" indicates how many major HO shells for single-particle basis, and "$N_{\rm max}$" is defined as the maximal allowed HO excitation above the lowest HO many-body configuration. The original interaction used is the NNLO$_{\rm opt}$ potential [23].

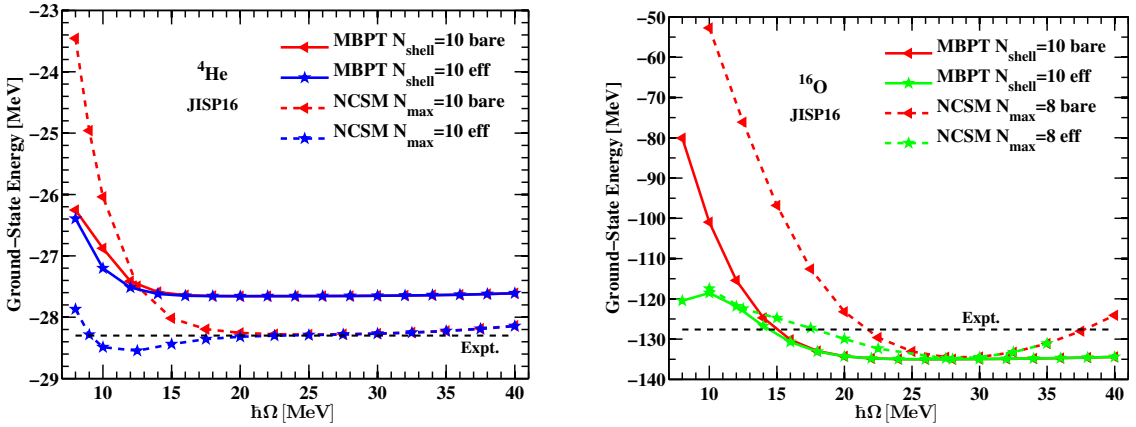

Fig. 6. (color online) Same as Fig. 5 but the original interaction used is the JISP16 potential [24–26].

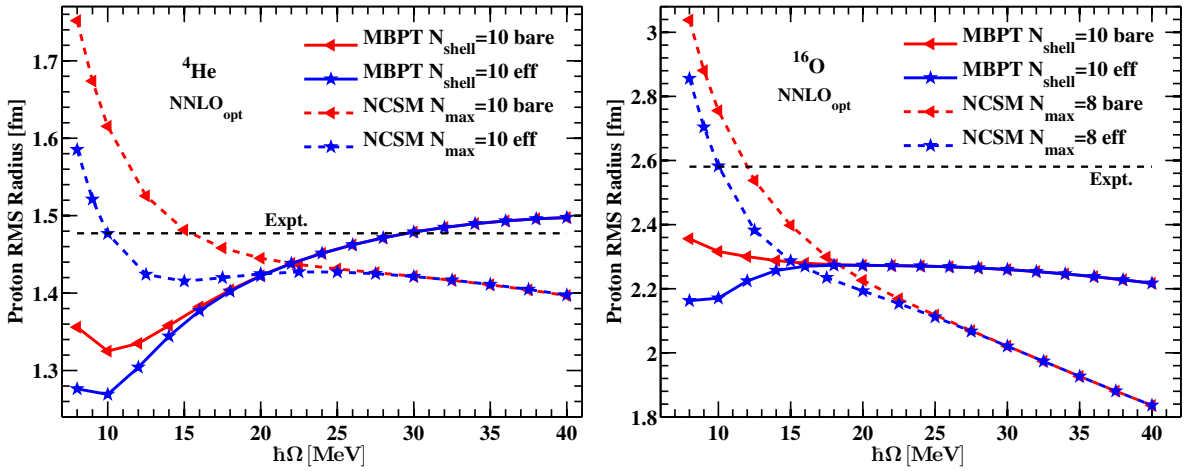

Fig. 7. (color online) Point-proton rms radii of ^{4}He and ^{16}O as a function of oscillator parameter $\hbar\Omega$ in MBPT and NCSM calculations. We calculate the one-body density for point-proton rms radii up to second order in MBPT, as shown in Ref. [51]. The original interaction used is the NNLO$_{\rm opt}$ potential [23].

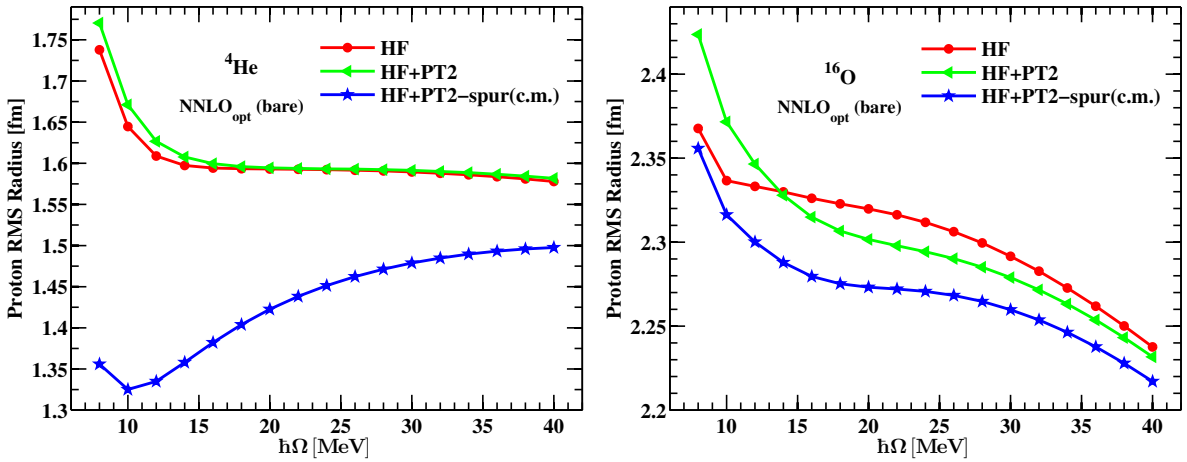

Fig. 8. (color online) Point-proton rms radii of ^{4}He and ^{16}O as a function of oscillator parameter $\hbar\Omega$ in MBPT calculations. The "PT2" in this figure denotes the second order of MBPT for one-body density, and "-spur(c.m.)" denotes the correction of spurious center-of-mass motion. The original interaction used is the NNLO$_{\rm opt}$ potential [23].

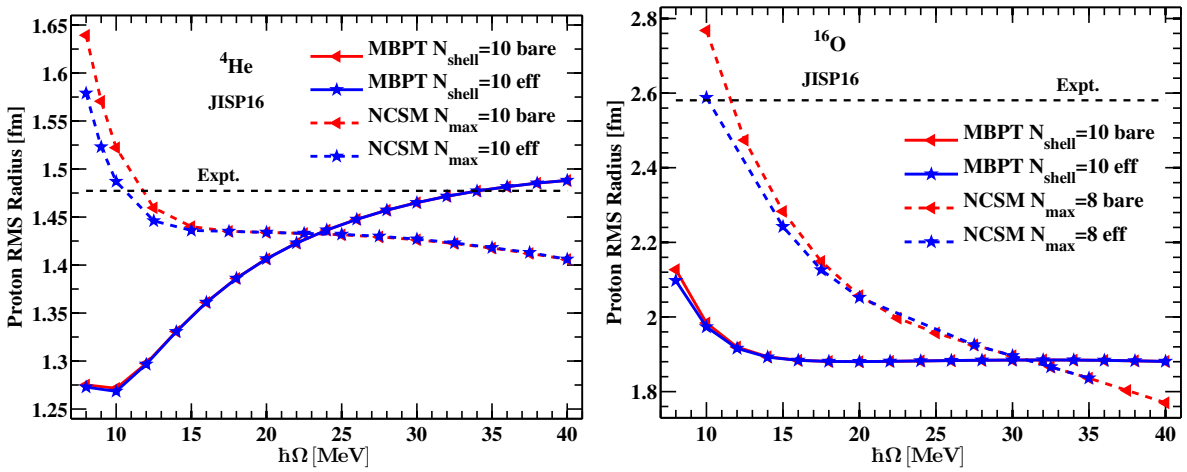

Fig. 9. (color online) Same as Fig. 7 but the original interaction used is the JISP16 potential [24–26].

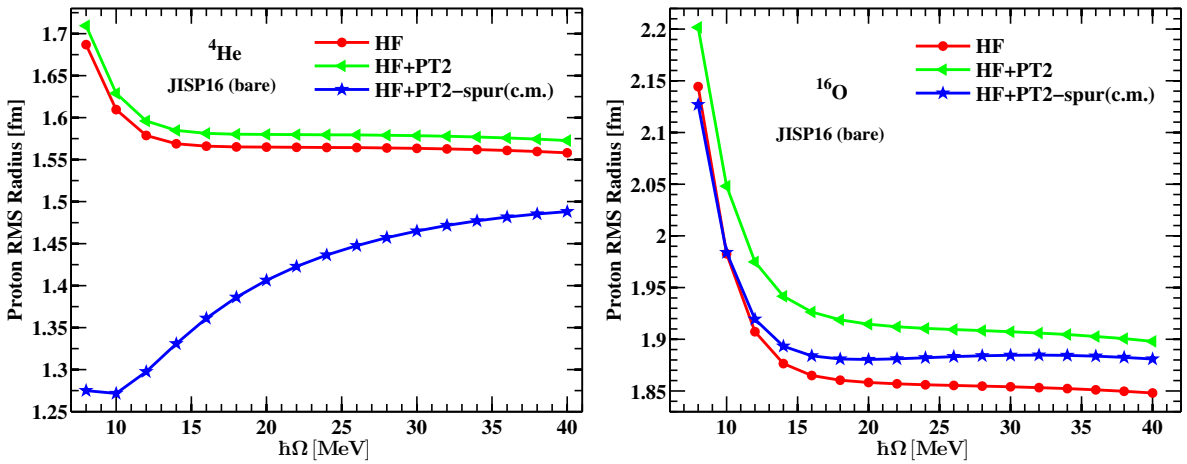

Fig. 10. (color online) Same as Fig. 8 but the original interaction used is the JISP16 potential [24–26].

interaction and "bare" interaction. For "harder" interactions, this value of $\hbar\Omega$ will be larger.

3.1.2 Root-mean-square radii

Our point-nucleon rms results of MBPT and NCSM are presented in Fig. 7. For this quantity, we found an interesting dependence on oscillator parameter $\hbar\Omega$ for different calculations in the same model spaces. In NCSM, the radii decrease with increasing $\hbar\Omega$, and this reflects the behavior of the HO basis states. However, we found that the MBPT calculation in HF basis improves convergence and reduces the frequency dependence compared to the NCSM calculation in HO basis, and there is a similar conclusion for NCSM using a natural orbital basis [52]. We also found that there is a strange curve where the radii increase with increasing $\hbar\Omega$ after a certain $\hbar\Omega$ for ^{4}He in MBPT. To interpret this trend, we look at the details of the MBPT calculation, as shown in Fig. 8. In this figure, the "HF" means the point-nucleon rms is calculated by HF one-body density, "HF+PT2" means taking into account the corrections of anti-symmetrized Goldstone diagram expansion in Rayleigh-Schrödinger perturbation theory for one-body density up to second order, and "-spur(c.m.)" denotes the correction of spurious center-of-mass motion. The correction of the rms radius for the spurious center-of-mass motion, $\Delta r_{\rm c.m.}$, is defined as [53]

$$\Delta r_{\rm c.m.}=[r^2_{\rm SHF}-\frac{b^2}{A}]^{1/2}-r_{\rm SHF}, \tag{33}$$

where $b^2=\frac{\hbar}{m\Omega}$ and A are the nucleon number. So, $\Delta r_{\rm c.m.}$ increases with increasing $\hbar\Omega$, and we can easily understand the trend of radii in MBPT. We also find that the point-nucleon rms results of HF has the same trend as the NCSM in the HO basis, and the higher corrections of MBPT for one-body density is very small.

3.2 Application to ^{40}Ca

Figure 11 shows the ground-state energy of ^{40}Ca in MBPT calculation as a function of $\hbar\Omega$ for different "bare" nuclear interactions and $N_{\rm shell}$ truncations. The convergence with the basis enlargement using the NNLO$_{\rm opt}$ potential is slower than with the JISP16 potential, and using the JISP16 potential has more overbinding energy than NNLO$_{\rm opt}$. We give some details about the ground-state observables of ^{40}Ca in Table 1 and 2 at the $\hbar\Omega$ where minimum energy is obtained. We conclude that the NNLO$_{\rm opt}$ potential can minimize the need for three-body force effects, and the JISP16 potential needs further phase-equivalent transformations or three-body forces for heavier nuclei.

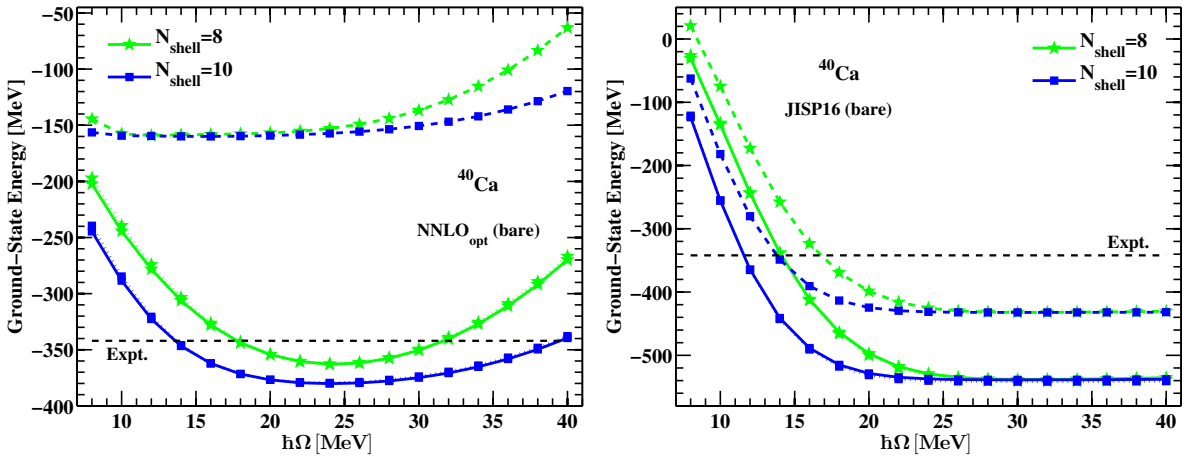

Fig. 11. (color online) Ground-state energies of ^{40}Ca as a function of oscillator parameter $\hbar\Omega$ in MBPT calculations with HF reference energy (long-dashed line), added second- (dashed line) and third-order (solid line) MBPT corrections. The original interactions used are the NNLO$_{\rm opt}$ potential [23] and JISP16 potential [24–26].

Table 1. Ground-state observables of ^{40}Ca with "bare" NNLO$_{\rm opt}$ interaction [23] ($N_{\rm shell}=10$ and $\hbar\Omega=24$ MeV).

observable	p-rms/fm	$E_{\rm g.s.}$/MeV
Expt.	3.39	-342.05
SHF	2.8382	-157.25
PT2	-0.0055	-222.18
PT3	–	-0.68
$\Delta r_{\rm c.m.}$	-0.0076	–
MBPT total	2.8251	-380.11

Table 2. Ground-state observables of ^{40}Ca with "bare" JISP16 interaction [24–26] ($N_{\rm shell}=10$ and $\hbar\Omega=30$ MeV).

Observable	p-rms/fm	$E_{\rm g.s.}$/MeV
Expt.	3.39	-342.05
SHF	1.8672	-432.20
PT2	0.0254	-109.38
PT3	–	2.87
$\Delta r_{\rm c.m.}$	-0.0092	–
MBPT total	1.8835	-538.72

4 Summary

In this work, starting from the "softer" NN interactions $\mathrm{NNLO_{opt}}$ and JISP16, we have compared results obtained from MBPT in HF basis with NCSM in HO basis. These two methods use different model space truncations, the $N_{\max}$ and N_{shell} truncations, but they are in reasonable agreement in "close" model space. We also have compared the results using "bare" force with OLS renormalized force. We find that the two-body OLS effective interaction always improves on the bare interaction results, in particular, for smaller spaces and lower HO frequencies.

We are grateful to Prof. James P. Vary at Iowa State University, USA for valuable discussions and providing the $NNLO_{opt}$ and JISP16 interactions.

References

1 P. Navrátil and B. R. Barrett. Phys. Rev. C, **57**: 562–568 (1998)
2 P. Navrátil, J. P. Vary and B. R. Barrett. Phys. Rev. Lett., **84**: 5728–5731 (2000)
3 B. R. Barrett, P. Navrátil and J. P. Vary. Progress in Particle and Nuclear Physics, **69(0)**: 131 – 181 (2013)
4 S. C. Pieper, V. R. Pandharipande, R. B. Wiringa and J. Carlson. Phys. Rev. C, **64**: 014001 (2001)
5 S. C. Pieper, R. B. Wiringa and J. Carlson. Phys. Rev. C, **70**: 054325 (2004)
6 M. Pervin, S. C. Pieper and R. B. Wiringa. Phys. Rev. C, **76**: 064319 (2007)
7 L. E. Marcucci, M. Pervin, S. C. Pieper, R. Schiavilla and R. B. Wiringa. Phys. Rev. C, **78**: 065501 (2008)
8 G. Hagen, T. Papenbrock, D. J. Dean and M. Hjorth-Jensen. Phys. Rev. Lett., **101**: 092502 (2008)
9 G. Hagen, T. Papenbrock and D. J. Dean. Phys. Rev. Lett., **103**: 062503 (2009)
10 G. Hagen, T. Papenbrock, D. J. Dean and M. Hjorth-Jensen. Phys. Rev. C, **82**: 034330 (2010)
11 R. Roth and P. Navrátil. Phys. Rev. Lett., **99**: 092501 (2007)
12 M. K. G. Kruse, E. D. Jurgenson, P. Navrátil, B. R. Barrett and W. E. Ormand. Phys. Rev. C, **87**: 044301 (2013)
13 L. Coraggio, N. Itaco, A. Covello, A. Gargano and T. T. S. Kuo. Phys. Rev. C, **68**: 034320 (2003)
14 Hasan, A. Mahmoud, J. P. Vary and P. Navrátil. Phys. Rev. C, **69**: 034332 (2004)
15 R. Roth, P. Papakonstantinou, N. Paar, H. Hergert, T. Neff and H. Feldmeier. Phys. Rev. C, **73**: 044312 (2006)
16 F. R. WANG, X. F. MENG, Y. A. LUO and F. PAN. Chinese physics C, **32(S2)**: 109 (2008)
17 F. Pan, V. G. Gueorguiev and J. P. Draayer. Phys. Rev. Lett., **92**: 112503 (2004)
18 S. G. Zhou, C. K. Zheng and J. M. Hu. Chinese physics C, **22(12)**: 1143 (1998)
19 Z. Z. Ren and G. O. Xu. Chinese physics C, **19(11)**: 1029 (1995)
20 S. G. Zhou, F. R. Xu, C. K. Zheng and J. M. Hu. Chinese physics C, **23(08)**: 803 (1999)
21 Y. M. Zhao, J. Q. Chen and B. Q. Chen. Chinese physics C, **21(04)**: 356 (1997)
22 Y. M. Zhao and A. Arima. Physics Reports, **545(1)**: 1 – 45 (2014)
23 A. Ekström, G. Baardsen, C. Forssén, G. Hagen, M. Hjorth-Jensen, G. R. Jansen, R. Machleidt, W. Nazarewicz, T. Papenbrock, J. Sarich and S. M. Wild. Phys. Rev. Lett., **110**: 192502 (2013)
24 A. M. Shirokov, A. I. Mazur, S. A. Zaytsev, J. P. Vary and T. A. Weber. Phys. Rev. C, **70**: 044005 (2004)
25 A. Shirokov, J. Vary, A. Mazur, S. Zaytsev and T. Weber. Physics Letters B, **621(1-2)**: 96 – 101 (2005)
26 A. Shirokov, J. Vary, A. Mazur and T. Weber. Physics Letters B, **644(1)**: 33 – 37 (2007)
27 I. Stetcu, B. Barrett and U. van Kolck. Physics Letters B, **653(2-4)**: 358 – 362 (2007)
28 R. J. Furnstahl, G. Hagen and T. Papenbrock. Phys. Rev. C, **86**: 031301 (2012)
29 S. A. Coon, M. I. Avetian, M. K. G. Kruse, U. van Kolck, P. Maris and J. P. Vary. Phys. Rev. C, **86**: 054002 (2012)
30 S. Ôkubo. Progress of Theoretical Physics, **12(5)**: 603–622 (1954)
31 K. Suzuki and S. Y. Lee. Progress of Theoretical Physics, **64(6)**: 2091–2106 (1980)
32 K. Suzuki. Progress of Theoretical Physics, **68(1)**: 246–260 (1982)
33 K. Suzuki and R. Okamoto. Progress of Theoretical Physics, **70(2)**: 439–451 (1983)
34 K. Suzuki. Progress of Theoretical Physics, **68(6)**: 1999–2013 (1982)
35 K. Suzuki and R. Okamoto. Progress of Theoretical Physics, **92(6)**: 1045–1080 (1994)
36 P. Navrátil and E. Caurier. Phys. Rev. C, **69**: 014311 (2004)
37 R. Machleidt. Phys. Rev. C, **63**: 024001 (2001)
38 V. G. J. Stoks, R. A. M. Klomp, C. P. F. Terheggen and J. J. de Swart. Phys. Rev. C, **49**: 2950–2962 (1994)
39 R. B. Wiringa, V. G. J. Stoks and R. Schiavilla. Phys. Rev. C, **51**: 38–51 (1995)
40 P. Doleschall. Phys. Rev. C, **69**: 054001 (2004)
41 D. R. Entem and R. Machleidt. Phys. Rev. C, **68**: 041001 (2003)
42 R. Machleidt and D. Entem. Physics Reports, **503(1)**: 1 – 75 (2011)
43 K. A. Brueckner. Phys. Rev., **97**: 1353–1366 (1955)
44 J. Goldstone. Proc. R. Soc. Lond. A, **239**: 267–279 (1957)
45 H. A. Bethe, B. H. Brandow and A. G. Petschek. Phys. Rev., **129**: 225–264 (1963)
46 S. Bogner, T. T. S. Kuo, L. Coraggio, A. Covello and N. Itaco. Phys. Rev. C, **65**: 051301 (2002)
47 S. Bogner, T. Kuo and A. Schwenk. Physics Reports, **386(1)**: 1 – 27 (2003)
48 S. K. Bogner, R. J. Furnstahl and R. J. Perry. Phys. Rev. C, **75**: 061001 (2007)
49 R. Roth, H. Hergert, P. Papakonstantinou, T. Neff and H. Feldmeier. Phys. Rev. C, **72**: 034002 (2005)
50 R. Roth, T. Neff and H. Feldmeier. Progress in Particle and Nuclear Physics, **65(1)**: 50 – 93 (2010)
51 B. S. Hu, F. R. Xu, Z. H. Sun, J. P. Vary and T. Li. Phys. Rev. C, **94**: 014303 (2016)
52 C. Constantinou, M. A. Caprio, J. P. Vary and P. Maris (2016)
53 J. W. Negele. Phys. Rev. C, **1**: 1260–1321 (1970)